1.55 Å Structure of the Ectoine Binding Protein TeaA of the Osmoregulated TRAP-Transporter TeaABC from *Halomonas elongata*[†,‡]

Sonja I. Kuhlmann,[§] Anke C. Terwisscha van Scheltinga,[§] Ralf Bienert,[||] Hans-Jörg Kunte,[||] and Christine Ziegler*[,§]

Department of Structural Biology, Max-Planck-Institute of Biophysics, Max-von-Laue-Strasse 3, 60438 Frankfurt am Main, Germany, Biology in Materials Protection and Environmental Issues, Federal Institute for Materials Research and Testing (BAM), Unter den Eichen 87, 12205 Berlin, Germany

Received April 16, 2008; Revised Manuscript Received June 26, 2008

ABSTRACT: TeaABC from the moderate halophilic bacterium *Halomonas elongata* belongs to the tripartite ATP-independent periplasmic transporters (TRAP-T), a family of secondary transporters functioning in conjunction with periplasmic substrate binding proteins. TeaABC facilitates the uptake of the compatible solutes ectoine and hydroxyectoine that are accumulated in the cytoplasm under hyperosmotic stress to protect the cell from dehydration. TeaABC is the only known TRAP-T activated by osmotic stress. Currently, our knowledge on the osmoregulated compatible solute transporter is limited to ABC transporters or conventional secondary transporters. Therefore, this study presents the first detailed analysis of the molecular mechanisms underlying substrate recognition of the substrate binding protein of an osmoregulated TRAP-T. In the present study we were able to demonstrate by isothermal titration calorimetry measurements that TeaA is a high-affinity ectoine binding protein ($K_d = 0.19\ \mu M$) that also has a significant but somewhat lower affinity to hydroxyectoine ($K_d = 3.8\ \mu M$). Furthermore, we present the structure of TeaA in complex with ectoine at a resolution of 1.55 Å and hydroxyectoine at a resolution of 1.80 Å. Analysis of the TeaA binding pocket and comparison of its structure to other compatible solute binding proteins from ABC transporters reveal common principles in compatible solute binding but also significant differences like the solvent-mediated specific binding of ectoine to TeaA.

The concentration of solutes (i.e., salt, sugar) in water determines the amount of water available to a cell. Adding salt or sugar to water leads to changes in the water's properties, such as osmotic pressure, which is caused by the decrease in the water's chemical potential (*1*). A nonadapted microorganism exposed to an environment like brine or sap must cope with its cytoplasmic water having a higher chemical potential than the surrounding water. Because water always flows from a higher to lower potential, a cell, with a membrane freely permeable to water will lose its cytoplasmic water until the potential gradient is abolished. In order to regain sufficient water required for growth, the cell must reduce the chemical potential of its cytoplasmic water. Many bacteria, archaea, and eukaryotic microorganisms achieve this through accumulation of large quantities of certain organic compounds, such as sugars, polyols, and amino acids and their derivatives, either by synthesis or by direct uptake from the environment (*2*−*5*). These nonionic, highly water-soluble molecules do not disturb the cell metabolism, even at high cytoplasmic concentrations, and are therefore called compatible solutes (*6*).

Many compatible solutes are beneficial for prokaryotic and eukaryotic cells not only as osmoregulatory solutes but also as protectants of proteins by mitigating detrimental effects of UV radiation, freezing, drying, and high temperatures. The beneficial effect is explained by the unfavorable interaction of compatible solutes with the protein backbone. The lower affinity of compatible solutes compared to water for the protein surface is termed the osmophobic effect and results in a thermodynamic force that contributes to protein folding and increased protein stability (*7, 8*).

The aspartate derivative ectoine is a widespread compatible solute among halophilic bacteria (*9*). Its protective properties in stabilizing enzymes and even whole cells make ectoine a valuable compound (*10*). Ectoine is marketed as an ingredient in skin-protecting cosmetics and has even attracted interest as a potential pharmaceutical (*11*). The halophilic γ-proteobacterium *Halomonas elongata* can tolerate salt concentrations well above 10% NaCl (*12*) and synthesize ectoine as its main solute. The biosynthesis proceeds via aspartic-semialdehyde, diaminobutyric acid, and N^{γ}-acetyldiaminobutyric acid (*7*). The enzymes required for ectoine synthesis in *H. elongata* are encoded by the genes *ectABC* (*13*). The hydroxylated derivative of ectoine, hydroxyectoine, is synthesized from ectoine by the ectoine hydroxylase EctD (*9*) (Figure 1).

H. elongata does not rely only on de novo synthesis of ectoine for adaptation to high saline environments but can also take up compatible solutes or precursors from the medium (*17*). To enable solute uptake, *H. elongata* is

[†] This work was funded by DFG KU 1112/3-1 and ZI 572/3-1.

[‡] The coordinate files of TeaA in complex with ectoine and in complex with hydroxyectoine were deposited in the Protein Data Bank with the file names 2vpn and 2vpo, respectively.

* To whom correspondence should be addressed. Telephone: +49 (69) 6303-3054. Fax: +49 (69) 6303-3002. E-mail: christine.ziegler@mpibp-frankfurt.mpg.de.

[§] Max-Planck-Institute of Biophysics.

[||] BAM.

10.1021/bi8006719 CCC: $40.75
Published on Web 08/15/2008

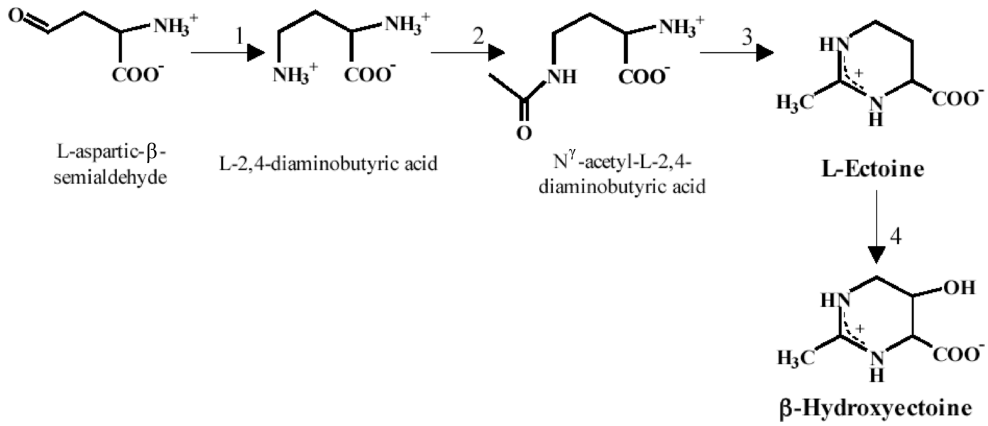

FIGURE 1: Biosynthetic pathway of the compatible solute ectoine (1,4,5,6-tetrahydro-2-methyl-4-pyrimidinecarboxylic acid) and hydroxyectoine based on enzymological and genetic studies (*13*−*16*): 1, L-2,4-diaminobutyric acid transaminase (encoded by *ectB*); 2, L-2,4-diaminobutyric acid N^{γ}-acetyltransferase (encoded by *ectA*); 3, ectoine synthase (encoded by *ectC*); 4, ectoine hydroxylase (encoded by *ectD*).

equipped with a set of compatible solute transporters of which only one accepts ectoine as substrate, namely, the ectoine-specific transporter for ectoine accumulation, TeaABC (*18*). TeaABC is not only required for the accumulation of external ectoine but also functions as a salvage system for ectoine leaking out of the cell (*18*). This observation led to the hypothesis that TeaABC might be involved in regulating the cytoplasmic ectoine concentration (*5*). TeaABC is a distinctive transporter in this respect and the first osmoregulated compatible solute transporter belonging to the family of tripartite ATP-independent periplasmic (TRAP)[1] transporters (*18*). TRAP transporters were characterized for the first time in *Rhodobacter capsulatus*, where a system called DctPQM has been shown to catalyze the nonosmoregulatory uptake of C4-dicarboxylates (*19*). Homologues of the TRAP DctPQM system of *Rhodobacter* have been identified in numerous Gram-negative and Gram-positive bacteria, as well as in archaea (*20, 21*). Similar to DctPQM, the osmoregulatory TRAP transporter TeaABC consists of three nonhomologous proteins (*18*): TeaC, a large transmembrane protein, TeaB, a small transmembrane protein, and TeaA, a periplasmic substrate binding protein (SBP) (*22*). Although the transport of substrates is mediated by an SBP similar to ATP-dependent ABC transporters, transport activity of TRAP systems is not linked to ATP hydrolysis but is coupled to the cotransport of ions (*19, 23*).

The unique organization of the TRAP-T transmembrane domain consisting of two proteins is explained by the need for a membrane-based partner protein for the periplasmic SBP (*21, 24*). Recently, the first crystal structures of SBPs belonging to the TRAP transporter family were determined, namely, SiaP from *Haemophilus influenzae* (*25*), DctP6 and DctP7 from *Bordetella pertussis* (*26*), TakP from *Rhodobacter sphaeroides* (*27*), TrGluBP from *Thermus thermophilus* (*28*), and a SBP from *Thermotoga maritima* (PDB entry 2hpg). SiaP and TakP are involved in the binding and transport of sialic acid and α-keto acids, respectively, while DctP6 and DctP7 facilitate the uptake of pyroglutamic acid. The structural analysis of Siap and TakP with and without their respective substrates bound revealed that these proteins follow the Venus fly trap mechanism observed in binding proteins from ABC transporters. None of these binding proteins of TRAP transporters are involved in osmoregulatory processes, as TeaABC is. The biological relevance of TeaA is more similar to EhuB, an SBP from the ABC transporter EhuABCD from *Sinorhizobium meliloti* (*29*). Although not synthesized to function at high salinities, EhuB is a compatible solute binding protein that enables the high-affinity uptake of ectoine and hydroxyectoine via the Ehu system (*29, 30*).

In order to gain a deeper insight into the structure−function relationship of SBPs from a TRAP system functioning at high salinity, we determined the X-ray structure of TeaA from *H. elongata* in complex with ectoine and hydroxyectoine at a resolution of 1.55 and 1.80 Å, respectively. Our studies revealed a monomeric structure of TeaA. A binding motif employing solvent as a "co-ligand" characterizes the binding site for ectoine in TeaA. The binding motif allows for the high-affinity binding of ectoine (K_d = 0.19 μM) exceeding the affinity of EhuB for ectoine. This finding is in agreement with the biological function of TeaABC that takes over the role as a transporter for exogenous ectoine and a salvage system for ectoine leaking out of the cell.

EXPERIMENTAL PROCEDURES

Purification of TeaA. The gene *teaA* (AY061646) was amplified from genomic DNA that was extracted from *H. elongata* (*31*) with the primers 5′-ggaaccacacatatgaaggcatacaagc-3′ and 5′-ggagaggcaagctttcagccctcgctctcgc-3′ using the GC-RICH PCR System (Roche Applied Science). The PCR product was cloned in the pET22b vector (Novagen) using the *Nde*I and *Hin*dIII restriction sites on vector and PCR product. The resulting vector pET22b-TeaA was transformed into *Escherichia coli* BL21(DE3) C41 cells (Avidis). Synthesis of TeaA was performed at 30 °C in M9 minimal medium after induction with 50 nM IPTG at an OD_{600} of 0.6. TeaA is exported into the medium as described by Tetsch and Kunte (*22*). Cells were discarded after 16 h growth and TeaA containing medium was purified by anion-exchange chromatography using Q-Sepharose (GE Healthcare). TeaA was eluted by a gradient from 360 mM to 1 M NaCl in 25 mM Tris-HCl, pH 7.5, and concentrated to 10−20 mg/mL. To complex TeaA with the ligand, it was incubated with an equimolar amount of ectoine or hydroxyectoine at 37 °C for 1 h.

[1] Abbreviations: TRAP-T, tripartite ATP-independent periplasmic transporter; ITC, isothermal titration calorimetry; Tea, transporter for ectoine accumulation; SBP, solute binding protein; SeMet, selenomethionine.

Sodium chloride was removed by size exclusion chromatography (Superdex 200) in 25 mM Tris-HCl, pH 7.5.

Selenomethionine-substituted (SeMet) TeaA was synthesized in methionine auxotroph BL21(DE3) codon plus RP-X cells. Purification was performed as described above in the presence of 2 mM DTT. Purity was about 98% after size exclusion chromatography as checked by SDS−PAGE. TeaA has a N-terminal leader sequence for the transport by the Sec pathway. The processed form of TeaA with 316 amino acid residues has a molecular mass of 36 kDa (*22*).

Isothermal Titration Calorimetry (ITC). TeaA was prepared as described above without the addition of ligand and rebuffered with 50 mM sodium phosphate buffer, pH 7.3, using dialysis tubes with 10 kDa molecular mass cutoff. The concentration was determined with the BCA protein assay microplate kit (Pierce, Bonn, Germany). Gravimetrically determined amounts of ligands were dissolved in the same buffer. Solutions were degassed under vacuum prior to use. Isothermal titration calorimetry was performed on a VP-ITC microtitration calorimeter from Microcal, MA (*32*), equipped with the VPViewer software and a origin-based software adapted to ITC measurements for data acquisition and analysis. In a typical titration experiment one injection of 3 μL and 28 injections of 10 μL of ligand solution (600 μM) were injected to the sample cell containing 1.42 mL of TeaA (61 μM). The first injection was not included in data processing. To ensure fast and complete mixing of the ligand and TeaA, the sample cell was stirred continuously at 307 rpm. Before injection the instrument was equilibrated to attain a stable baseline at the desired temperature at 25 °C if not indicated otherwise. Control experiments to verify the heat of dilution were performed by titrating ligand to buffer. The heat of dilution for ectoine or hydroxyectoine pipetted in buffer was considered to be negligible and not included in data processing. Each experiment consists of three independent measurements.

3D Crystallization. Initial crystallization conditions were found by Hampton I, II, and Index screen in Greiner 96 three-well sitting drop plates using a Cartesian pipetting robot. All crystallization trials were performed at 18 °C with a protein concentration of about 60 mg/mL as determined by the Bradford protein assay (Sigma). Usually crystals grew within 5 days. Crystals of TeaA in complex with ectoine grew in 0.1 M HEPES, pH 8.0, 0.1 M $MgCl_2$, and 30% PEG 3350 in sitting drops. Those crystals in complex with hydroxyectoine were obtained in similar conditions as for ectoine crystals, but with 0.04 M $MgCl_2$ and 35% PEG 3350. Crystals of SeMet-derivatized TeaA in complex with ectoine were obtained by microseeding in a hanging drop in 0.1 M Hepes, pH 7.5, 0.1 M $MgCl_2$, and 25.5% PEG 3350.

Data Collection, Structure Determination, and Refinement. For data collection the crystals were flash frozen without additional cryoprotectant in liquid nitrogen. All data were collected at beamline PXII at the Swiss Light Source (SLS). The data were reduced and scaled with the programs XDS and XSCALE (*33*). For the SeMet data the positions of selenium sites were determined with the program HKL2MAP (*34*). Refinement of the sites and first automated model building with native data of crystals of TeaA in complex with ectoine were done with AutoSHARP (*35*) and ARP/wARP (*36*). Iterative rounds of manual building in COOT followed by refinement with REFMAC5 (*37*) improved the initial model to the final one. The structure of TeaA with hydroxyectoine was solved with rigid body refinement of the polypeptide of ectoine structure. The restraint dictionaries of ectoine and hydroxyectoine were built with Sketcher from the CCP4i suite (*38*) as described from Cialla et al. (*39*). All molecular drawings were produced with Pymol (*40*).

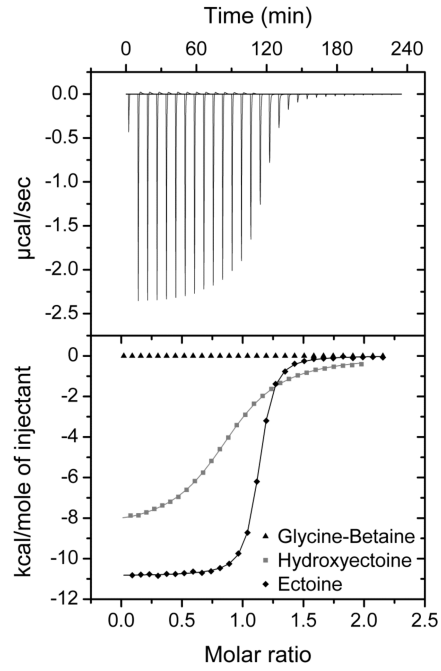

FIGURE 2: Typical ITC raw data for binding of ectoine to TeaA (upper panel) and integrated ITC curves (lower panel) for the binding of glycine-betaine (triangles), hydroxyectoine (squares), and ectoine (diamonds) to TeaA, respectively, and corresponding fits (solid lines) considering a one-site binding model.

Sequence and Structure Alignments. A search for similar structures to TeaA was done with DALI (*41*). RMSD values and rotation axes were determined with LSQKAB (*42*) of the CCP4 suite (*38*). Sequences of putative ectoine binding proteins were found with BLAST (*43*) and aligned with ClustalW (*44*). Sequence alignment was drawn with Bioedit (*45*) and ESPript (*46*).

RESULTS AND DISCUSSION

TeaA Is a High-Affinity Ectoine Binding Protein. Thermodynamic parameters for the binding of TeaA to ectoine, hydroxyectoine, and glycine-betaine were determined by isothermal titration calorimetry (ITC). The binding of ectoine and hydroxyectoine to TeaA shows exothermic signals with a stochiometry factor corresponding to 1 using a one-site binding model. Both interactions are enthalpy driven with an unfavorable entropic contribution (Figure 2 and Table 1). TeaA binds ectoine with high affinity, and a dissociation constant (K_d) of 0.19 μM was determined. In contrast, the affinity for hydroxyectoine is approximately 20-fold lower with a K_d value of 3.8 μM. This is reflected by an increase of free energy of 1.8 kcal/mol arising solely from decreased enthalpy, from ΔH of −11.5 to −8.6 kcal/mol. The entropical contribution for the binding of hydroxyectoine to TeaA is with a $T\Delta S$ value of −1.2 kcal/mol even less unfavorable than the binding of ectoine with a $T\Delta S$ value of −2.4 kcal/mol (Table 1). Titration of glycine-betaine to TeaA at 25 °C (Figure 2) and 5 °C (data not shown) revealed small peaks

Table 1: Thermodynamic Parameters of Ligand Binding to TeaA[a]

ligand	K_a (μM^{-1})	K_d (μM)	ΔG (kcal/mol)	ΔH (kcal/mol)	$T\Delta S$ (kcal/mol)	n
ectoine	5.19 ± 0.44	0.19 ± 0.02	-9.15 ± 0.05	-11.52 ± 0.57	-2.37 ± 0.62	1.0 ± 0.1
hydroxyectoine	0.26 ± 0.05	3.80 ± 0.07	-7.39 ± 0.01	-8.57 ± 0.01	-1.18 ± 0.02	0.9 ± 0.0

[a] Each measurement represents the mean value of three independent measurements.

Table 2: X-ray Data Collection, Refinement, and Model Statistics

Crystal Data	selenomethionine derivative		
cell dimensions (Å; deg)	$a = 48.8$, $b = 52.3$, $c = 63.8$; $\alpha = 80.5$, $\beta = 85.6$, $\gamma = 77.7$		
space group	*P*1	*P*1	*P*1
Data Collection	remote	peak	inflection
wavelength (Å)	0.9765	0.9798	0.9801
resolution[a] (Å)	47−2.15 (2.25−2.15)	60−2.15 (2.25−2.15)	60−2.15 (2.25−2.15)
no. of observed reflections	307012 (9595)	258399 (7442)	106156 (3168)
no. of unique reflections[a]	58013 (3325)	57634 (3055)	56822 (3052)
completeness[a] (%)	89.5 (40.1)	88.9 (36.9)	87.7 (36.8)
I/σ[a] (I)	15.8 (4.0)	13.96 (3.72)	7.91 (1.74)
R_{meas}[a,b] (%)	9.7 (30.6)	9.8 (29.6)	10.6 (58.0)
MAD phasing power iso/ano[c]	na/0.934	0.618/1.127	0.425/0.396
MAD phasing figure of merit	0.445		
Crystal Data	ectoine	hydroxyectoine	
cell dimensions (Å; deg)	$a = 48.3$, $b = 52.2$, $c = 63.5$; $\alpha = 80.8$, $\beta = 85.8$, $\gamma = 77.9$	$a = 48.6$, $b = 52.1$, $c = 63.7$; $\alpha = 80.8$, $\beta = 85.7$, $\gamma = 78.0$	
Data Collection	*P*1	*P*1	
wavelength (Å)	0.9781	0.9789	
resolution[a] (Å)	20−1.55 (1.65−1.55)	20−1.80 (1.84−1.80)	
no. of observed reflections[a]	251318 (25830)	207782 (11881)	
no. of unique reflections[a]	81024 (13680)	53752 (3315)	
completeness[a] (%)	93.3 (92.3)	96.2 (94)	
I/σ[a] (I)	9.2 (2.3)	8.83 (2.39)	
R_{meas}[a,b] (%)	9.3 (47.5)	14.3 (81.7)	
Refinement			
resolution (Å)	1.55	1.80	
R_{work} (98% of total reflections) (%)	15.8	17.9	
R_{free} (2% of total reflections) (%)	20.3	22.5	
no. of protein atoms	4977	5292	
no. of ligand atoms	10	11	
no. of solvent molecules	659	301	
no. of magnesium ions	8	2	
RMSD[d] from ideal bond length (Å)	0.01	0.01	
RMSD[d] from ideal bond angles (deg)	1.3	1.4	
average *B* factor model atoms (Å^2)	16.5	16.8	
Wilson *B* factor (Å^2)	20.9	24.8	
Ramachandran plot favored (%)	93.7	93.7	
Ramachandran plot allowed (%)	6.3	6.3	

[a] Data in parentheses represent highest resolution shell. [b] For definition of R_{meas} see Diederichs, K., and Karplus, P. A. (1997) Improved R-factors for diffraction data analysis in macromolecular crystallography, *Nat. Struct. Biol. 4*, 269−275. [c] na, not applicable. [d] RMSD, root mean square deviation.

identified as dilution peaks, but no binding of glycine-betaine to TeaA could be determined (Figure 2). In addition, specificity of TeaA to ectoine was tested by a modified retention HPLC assay with alanine and proline (*14*, *15*) as control. It can be concluded that TeaA is a specific, high-affinity ectoine and hydroxyectoine binding protein.

Overall Structure of TeaA. TeaA in complex with ectoine or hydroxyectoine crystallizes in space group *P*1. The three-dimensional structure of TeaA in complex with ectoine was determined using the multiple-wavelength anomalous dispersion (MAD) method with a SeMet derivative refined against native data to 1.55 Å resolution. The inflection data set, as taken as last, suffered from radiation damage reflected by an R_{meas} of 58% (Table 2). The positions of 20 selenium sites were found immediately with the program HKL2MAP. After refinement of the sites and processing with AutoSHARP about 80% of the sequence was traced automatically. Refinement and manual building improved the initial model to a resolution of 1.55 Å with R_{work} of 15.8% and R_{free} of 20.3%. The structure of TeaA in complex with ectoine displays two TeaA monomers with 310 residues and one ectoine each, 659 solvent molecules, and 8 magnesium ions in the unit cell. The structure of TeaA in complex with hydroxyectoine to 1.8 Å was solved via rigid body refinement of the ectoine structure (Table 2). The refined model with R_{work} of 17.1% and R_{free} of 22.4% has the same overall fold like the ectoine structure. The two monomers with 310 residues each have both one hydroxyectoine bound. There are 301 solvent molecules and 2 magnesium ions in the unit cell. In both structures the C-terminus is disordered from residue 311 to 316. Residues 42 to 46 are disordered in one monomer (A) of the asymmetric unit but ordered in the other monomer (B), due to stabilizing crystal contacts. Main crystal contacts are mediated via Mg^{2+} ions added prior to crystallization. Eight ions in the structure of TeaA in complex with ectoine and two in that with hydroxyectoine were unambiguously identified by their hexagonal coordination. They form crystal contacts directly to protein atoms or via solvent molecules. Notably, one magnesium ion has a key role in connecting residues Ala259 of monomer A and Gly55 of monomer B in both structures. Main crystal contacts are also formed by Mg^{2+} ions being coordinated by residues Glu255

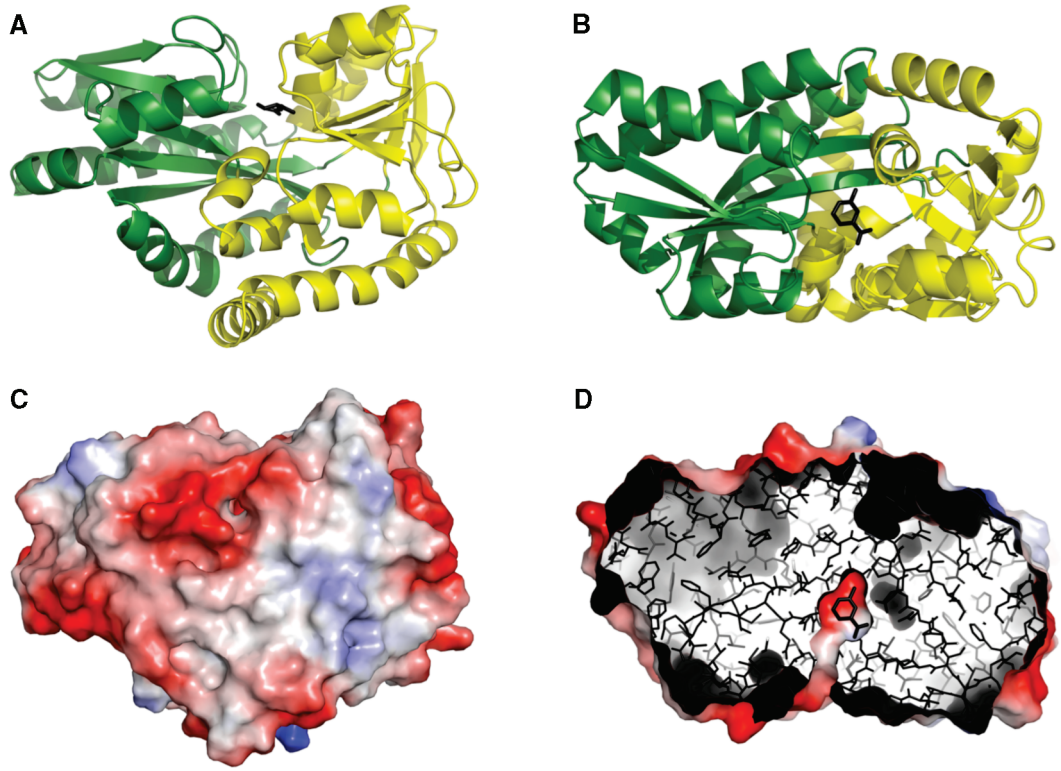

FIGURE 3: Overall structure of monomer B of the TeaA/ectoine complex. (A, B) TeaA shown as spiral model with an ectoine molecule (black) bound to the protein between domain 1 (residues 2−120 and 208−222, colored in green) and domain 2 (residues 121−207 and 258−302, colored in yellow). (C, D) Corresponding views of the electrostatic potential surface plot, with negative charges indicated in red and positive charges indicated in blue, show that TeaA is highly negatively charged. (D) The view in the interior of the proteins reveals ectoine fitting perfectly to the binding pocket, leaving just a narrow connection to the solvent surrounding the protein.

(monomer A) and Glu286 (monomer B) and Asn140 (monomer A) with Asp88 (monomer B). It can be assumed that ectoine or hydroxyectoine binding is not Mg^{2+} dependent, because no Mg^{2+} was detected in the binding pocket.

The structure of TeaA shares the major features of substrate binding proteins (SBPs) possessing two distinct globular α/β domains separated by a deep cleft (Figure 3A,B). Domain 1 stretches from residues 2 to 120 and 208 to −222 while domain 2 comprises residues 121−207 and 261−302. Domain 1 is composed of a five-stranded mixed β-sheet (β2-β1-β3-β10-β4) surrounded by five α-helices (α1, α2, α3, α4, α8), where β10 runs antiparallel to the other β-strands. Domain 2 comprises six α-helices (α5, α6, α7, α9, α10, α11) enclosing a six-stranded mixed β-sheet with the topology β7-β6-β8-β5-β9-β11 and β5 oriented in opposite direction to the others. The N-terminus linked to β1 is located in domain 1, whereas the C-terminus can be found in domain 2. The two domains are hinged together by a set of α-helices (α8-9) and two sets of β-sheets (β10-9 and β5-4), and the cleft formed between them constitutes the ligand binding site. Helices 9−11 fold across the base of the molecule and pack against both domains, with helices 8 and 9 spanning the whole molecule.

TeaA Is Adapted to High Salt Concentrations. The calculation of the surface potential indicates clearly a pronounced negative surface charge for TeaA (Figure 3C, and sequence analysis shows an acidic character of TeaA due to an excess of 42 acidic (Asp/Glu = 61) over basic (Arg/Lys = 19) residues. The acidic nature and exposure of the negative charge to the surface are common among proteins of extremely halophilic archaea (*19, 47*) that maintain high salt concentrations inside their cytoplasm with potassium and chloride being the dominating ions. The predominance of charged amino acids on the surface of enzymes is thought to stabilize their tertiary structure when exposed to high ionic surroundings (*48*−*51*). Extracellular proteins of halophilic bacteria, even those accumulating compatible solutes and keeping the intracellular salt concentration low, show an excess of acidic amino acids as known from proteins of extreme halophilic archaea.

The negative surface charge of TeaA (p*I* 4.14; net charge −42) is similar to those of extracellular proteins from halophilic bacteria (e.g., *Halomonas meridiana* amylase: p*I* 4.65; net charge −32) and extreme halophilic archaea (*Natrialba asiatica* serine protease: p*I* 4.11; net charge −49; *Natronococcus* sp. amylase: p*I* 4.12; net charge −82) (*52*), suggesting that TeaA is specifically adapted to high salt concentrations. In those halophilic bacteria performing osmoregulation by compatible solute accumulation, homologues of TRAP transporters and their corresponding TeaA were found, which exhibit most likely a similar negative surface potential.

TeaA Is a Type II SBP. The ectoine/TeaA complex displays a closed conformation, which is characteristic for periplasmic binding proteins in their ligand-bound state. The organization of the two hinged domains relative to each other allows for the characteristic "Venus fly trap" mechanism (*53*) of SBPs. This hinge-bending conformational change involves a significant rotation of single backbone torsion around the hinge region by which the open form of the protein closes around its ligand.

The domain topology (Figure 4) shows a dislocation of one β-strand in each β-sheet. This dislocation occurs at the joint position between domains 1 and 2 when the respective

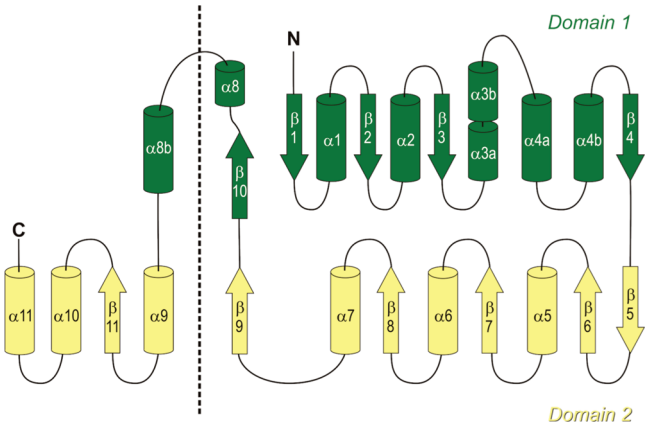

FIGURE 4: Topology of TeaA. Helices are represented with barrels and β-strands with arrows. The amino and carboxytermini are indicated with N and C, respectively. Structure elements homologous to ABC transporter binding proteins are located right of the dotted line, whereas structure elements left of the dotted line indicate evolutionarily unique structural features attributed exclusively for TRAP transporters.

β-strand adapts to the orientation of the corresponding strand in the other domain. SBPs have been classified into two groups depending on the topology of the β-sheets present in the two globular domains (*54*). Based upon this classification, TeaA is a member of the type II SBP (also called ESR for extracytoplasmic solute receptor) family, as it displays two domain crossovers involving strands β5 and β10 and a domain dislocation of one of the β-strands in each of the β-sheets.

A comparison of the three-dimensional structure of TeaA against the Protein Data Bank with DALI indicates a high similarity with a large number of SBPs, mainly from ABC transporters in their ligand-bound state and to four of the six currently available structures of TRAP-T SBPs. Structural similarity was found for the recently published structures of DctP6 and DctP7 (*26*), two homologous SBPs from *B. pertussis*, to SiaP from *H. influenzae* (*25*), and to the SBP of *T. maritima* (PDB entry 2hpg).

Compared to the topology of ABC type II SBPs TeaA has an additional structural element which is unique for TRAP-T SBPs and was also found in SiaP, DctP6, DctP7, and TakP (*25*−*27*). Located after the C-terminal part of domain 1, both domains are linked together by two to three α-helices separated by a short β-strand being parallel to the last β-strand of domain 2. This tight conformation may limit the flexibility of the opening movement and increase the rigidity of the whole Venus fly trap mechanism of SBPs of TRAP-Ts compared to that of type II SBPs of ABC transporters. The exposed and separated position of this additional structural element in all structures of TRAP-T SBPs supports the hypothesis that they have evolved from an ancestral type II SBP which was modified to specifically catalyze uptake of organic solutes with high affinity (*25*) and to bind to TRAP-T systems.

Substrate Binding Site. The structure of TeaA was solved in complex with ectoine and hydroxyectoine, compounds with similar chemical structure. The analysis of the $2F_o - F_c$ and $F_o - F_c$ electron density maps could unambiguously identify ectoine and hydroxyectoine. Both substrates are tightly bound to the protein, and there is just a narrow channel connecting the binding pocket with the solvent surrounding the protein (Figure 3D).

Ectoine binding in TeaA (Figure 5A,B) is mediated by a salt bridge to Arg144 and by hydrogen bonds to Glu9 and Asn184. Arg144 is the only highly conserved residue in TRAP-T SBPs and is found in all of the four structures of TRAP-T SBPs coordinating the carboxyl group of the substrates (*25*−*27*).

In addition, ectoine is sandwiched through van der Waals interactions in an aromatic binding pocket involving residues Trp188, Phe66, and Phe209. Trp188 is forming a cation−π interaction with the delocalized positive charge in ectoine. Residues Phe187 and Trp167 stabilize the aromatic box around ectoine, with Trp167 forming a $\pi-\pi$ interaction to Trp188 (Figure 5B). Phe209 is stabilized by van der Waals contacts to Met146 as well as Phe187 to Met124. Asn184 is hydrogen bonded to Gln15, Glu121, and Gln182 as well as Arg144 to the main chain nitrogen of Leu165.

The hydroxyectoine binding pocket (Figure 5C,D) is similar to that of ectoine but shows an altered hydrogen-bonding network; e.g., one solvent molecule exhibits a double conformation $W_a \leftrightarrow W_b$ (Figure 5A) in the ectoine binding site that is fixed in the hydroxyectoine binding pocket. Instead of contributing to the binding of the carboxyl moiety, the solvent molecule is now bound to the additional hydroxyl group of hydroxyectoine via a hydrogen bond.

Notably, loop 2 from residues 43 to 46 containing these important residues appears extremely flexible and is only resolved in monomer B due to stabilizing crystal contacts. Therefore, binding interactions of ectoine and hydroxyectoine shown in Figure 5A,C display one possible conformation of this loop segment (residues Glu44 and Ser45). Nevertheless, the pattern of solvent molecules can be traced back also in monomer A. It can be speculated that this flexible loop plays a role in the translocation of the ligand from TeaA to the transporter unit TeaBC. Further structural and functional studies on the whole transporter TeaABC together with site directed mutagenesis studies in this loop region of TeaA are required.

Comparison of TeaA with SBPs Specific for Ectoine and Glycine-Betaine. A BLAST was performed to identify putative ectoine TRAP transporters and their binding proteins. The BLAST was executed against the sequence of TeaC, because the transporter unit (DctM) represents the highest conserved part in the TRAP transporter complex. Organisms were chosen with respect to the role of ectoine as the main compatible solute and their capability of ectoine synthesis. *Chromohalobacter salexigens* is a close relative to *H. elongata* and its DctP exhibits a sequence identity of 33% to TeaA. The DctP proteins from *Halobacillus halophilus* and *Bacillus halodurans* show comparable identity levels of 35% and 34%, respectively. The highest sequence identity of 82.1% was found for DctP from the γ-proteobacterium *Marinobacter aquaeolei*. An alignment of these four putative ectoine binding proteins is shown in Figure 6 with the structural elements of TeaA displayed on top of the TeaA sequence. It reveals that charged residues involved in ectoine binding, Glu8-9 and Arg144, are highly conserved. Interestingly, Trp188, forming the strong cation−π interaction with ectoine, is not conserved and replaced by phenylalanine or alanine. Phe187 is highly and Phe209 is mostly conserved; the latter can also be replaced by tyrosine. Asn184

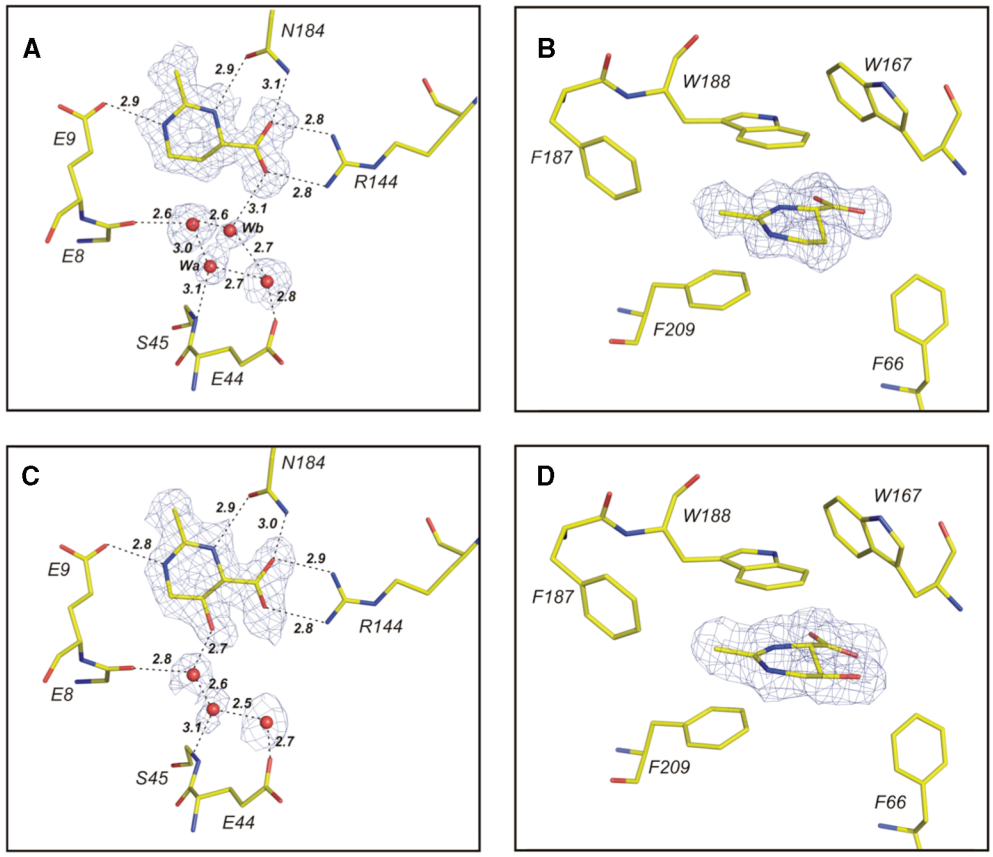

FIGURE 5: Architecture of the binding site of TeaA/ectoine as top view (A) and as corresponding side view (B) and structure of the binding site of TeaA/hydroxyectoine (C, D). The substrates ectoine and hydroxyectoine and the interacting amino acids are drawn by stick representation; solvent molecules are shown in red. W_a and W_b indicate low occupancy electron density regions, which are most likely populated by a water molecule oscillating between the two sites. The $F_o - F_c$ omit map of the solvent molecules and the substrates contoured at 2.0σ is displayed in blue. Dotted lines indicate hydrogen bonds and the numbers their length in Å. The orientation of residues Ser45 and Glu44 is one of several possible conformations. These residues are only ordered in monomer B, but not in monomer A.

is replaced by glutamine in two organisms. Only the nonconserved aromatic residue Trp188 is located in an α-helical part of the structure; the others are located in β-strands or in the adjacent loop before the next α-helical segment. The highly conserved glutamate cluster (Glu 8-9) is positioned in the center of the TeaA structure.

Most interestingly, the highly conserved arginine residues are all located in that region. The other residues involved in ligand binding are located in both domains for TeaA and $ProX_{Af}$ whereas in EhuB they are arranged concentrated in domain 1. In all three structures, the observed protein−ligand interactions have different degrees of asymmetry in domain population (EhuB (6:1), TeaA (2:4), and $ProX_{Af}$ (4:4)). In EhuB a single interaction of the bound ligand with domain 2 is enough to shift the equilibrium from the open conformation to the closed conformation of the Venus fly trap, while in TeaA this is caused by two interactions with domain 1. The consequences of such a highly asymmetrical distribution of residues involved in substrate binding are mentioned already in (*30, 55*) but are not completely understood up to now.

Interestingly, all of these structures (irrespective of their bacterial or archaeal origin) reveal similar solutions for binding of compatible solutes that are normally excluded from protein surfaces. Substrate binding is stabilized via salt bridges and/or hydrogen bonds and cation−π interactions between a special set of aromatic residues and the delocalized positive charge of the substrate. However, each protein has its own architecture of the substrate binding site. In EhuB the delocalized positive charge of the ligand interacts via cation−π interactions with three aromatic amino acid residues, two phenylalanines and a tyrosine. The binding of ectoine or hydroxyectoine in TeaA follows the described principle of compatible solute binding. A salt bridge and hydrogen bonds bind ectoine. Aromatic residues sandwich the ligand with cation−π and van der Waals interactions in the ligand binding site.

To compare the ligand binding of EhuB and TeaA, the ectoine molecules of both structures were overlaid and shown together with the aromatic residues of the binding pockets in Figure 7. The overlay reveals significant differences of ligand binding in EhuB and TeaA. However, the principal hydrogen bonds to ectoine and the coordination of the delocalized positive charge of the ligands via cation−π interactions are comparable in both structures. Arg144-TeaA and Arg85-EhuB form a similar salt bridge to the carboxyl group of ectoine in the same orientation. Glu 9-TeaA and Glu21-EhuB exhibit different orientations but a comparable hydrogen bond in both structures. Both binding pockets contain two phenylalanines. The aromatic amino acids Phe24, Tyr60, and Phe80 in EhuB correspond to the amino acids Phe187, Phe209, and Trp188 in TeaA, respectively. All hydrogen bonds in TeaA have a comparable counterpart in EhuB with similar length and angles and therefore also comparable binding energy. However, the carboxyl group of ectoine in TeaA forms hydrogen bonds to three amino

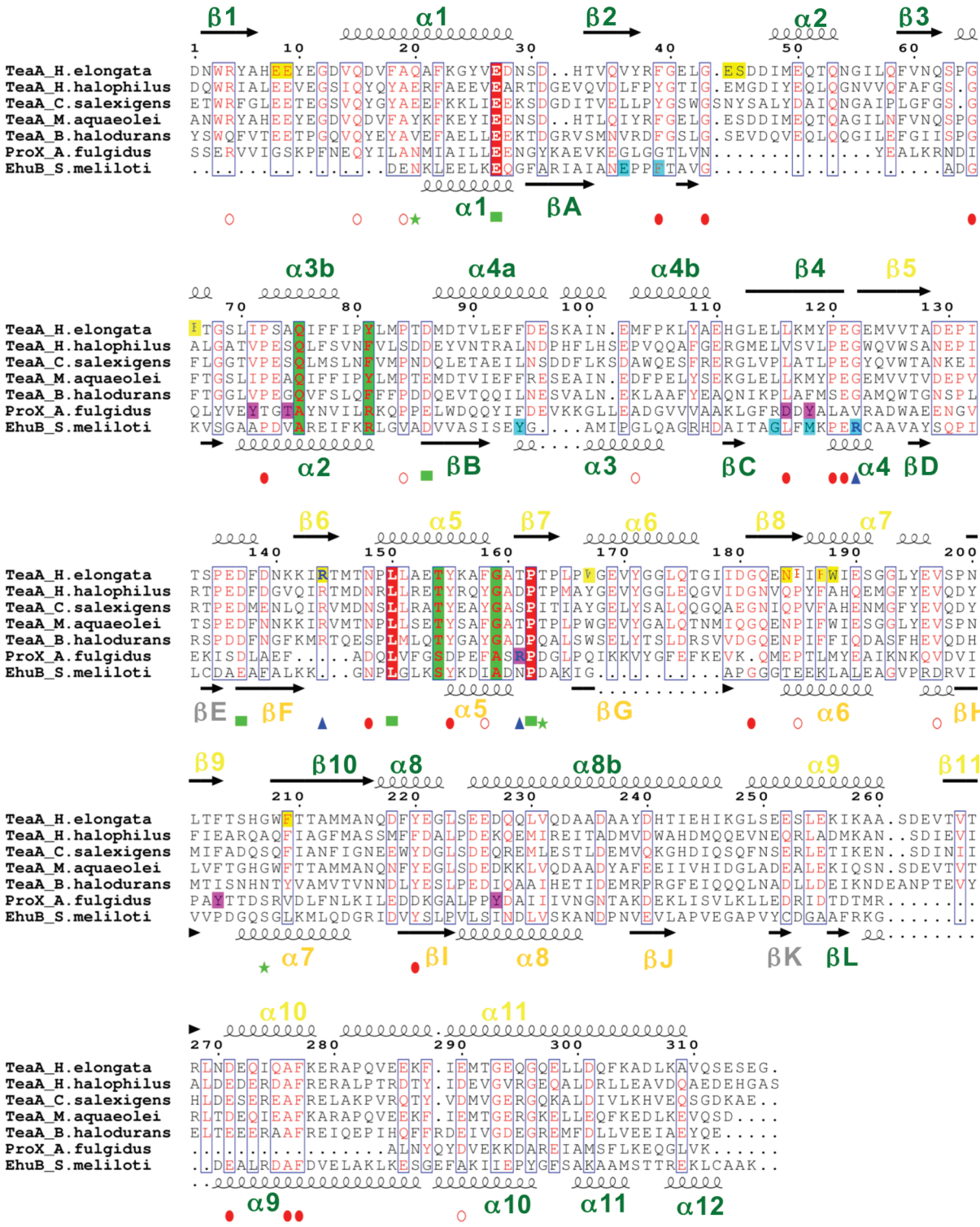

FIGURE 6: Sequence alignment of TeaA with selected putative TRAP transporter ectoine binding proteins, identified by a BLAST search against the corresponding transporter unit TeaC (proteins are named TeaA to simplify matters), and the glycine-betaine/proline-betaine binding ProX from *A. fulgidus* and the ectoine binding protein EhuB from *S. meliloti*. Structural elements of TeaA are shown on top of the TeaA sequence following the color coding of Figure 3A to distinguish between the domains and of EhuB below the EhuB sequence (color coding was adopted from ref *25*). Conserved residues in all proteins are highlighted in red and labeled (●), and residues that are separately conserved in TRAP transporters and ABC transporters are highlighted in green; blue boxes indicate a 65% consensus in the multiple sequence alignment. Residues involved in ligand binding are highlighted in yellow (TeaA), magenta (ProX), and cyan (EhuB). Arginines highly conserved in the binding pocket of all SBPs are colored in blue and labeled (▲). Different labels show residues which are conserved simultaneously in TeaA and EhuB (○), in TeaA and ProX (★), and in EhuB and ProX (■).

acid residues in contrast to four amino acid residues in EhuB. In TeaA the fourth hydrogen bond is established with a water cluster inside the binding pocket (Figure 5C). This feature is new for compatible solute binding proteins and contradicts the hypothesis that ligand binding site architectures of SBPs involved in osmoprotection are optimized for selectivity without relying on additional "co-ligands" such as water molecules (*30*).

Ligand binding affinities of EhuB determined with tryptophan quenching have K_d values of 1.6 and 0.5 μM for

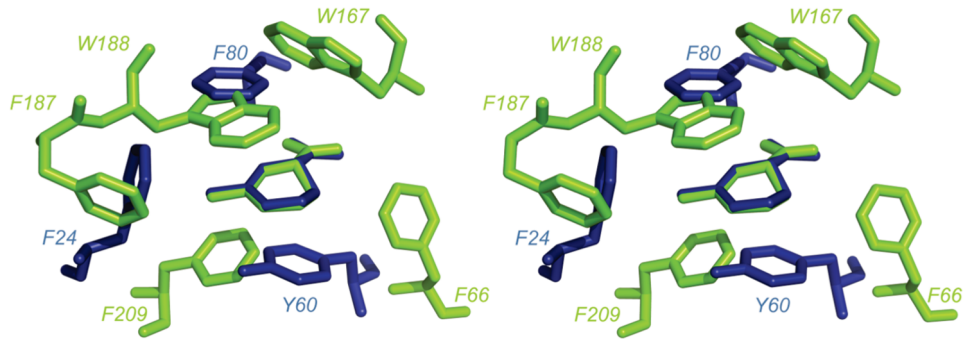

FIGURE 7: Stereoview of the ectoine binding sites of TeaA (green) and EhuB (blue), displaying the aromatic residues. Both ectoines were superimposed.

ectoine and hydroxyectoine, respectively. The contribution of individual amino acid residues involved in ligand binding in EhuB was investigated by site-directed mutagenesis to gain insights into their role in complex stabilization by measuring the steady-state affinities of ectoine and hydroxyectoine. Phe80 was found to be very important for stabilizing the bound ligand. Increasing the strength of the cation$-\pi$ interaction by placing a tyrosine or tryptophan at position 24 or 80, or a tryptophan at position 60, creates a protein with a 10−50-fold higher affinity (*30*). Interestingly, this result is in clear contrast to $ProX_{Ec}$ (*56*) where a substitution of any tryptophan with an aromatic amino acid is tolerated within the tryptophan box without significantly altering the affinity of the ligand.

An inherent problem of this strategy of mutating residues, especially in tightly constructed binding sites, is that substituting a residue might cause structural changes that in turn can affect the affinity of the mutant protein for its ligands. As a matter of fact, TeaA exhibits a Trp188 at the same position as Phe80 within the ligand binding site in EhuB, which would correspond to the mutation F80W, with an affinity of 0.02 μM to ectoine. Compared to the wild-type EhuB (1.6 μM) the affinity of TeaA to ectoine (0.2 μM) is indeed elevated. TeaA has, compared to EhuB, a higher amount of aromatic residues in the binding pocket (Figure 7). This can be an additional reason for the higher binding affinity of TeaA to ectoine compared to EhuB.

The binding of hydroxyectoine in TeaA shows a different water cluster compared to the binding of ectoine (Figure 5). While a solvent molecule is involved in binding to the carboxyl group of ectoine, the additional hydroxyl group expels this solvent molecule when hydroxyectoine is attached to the binding pocket. Instead, another solvent molecule of the cluster forms a hydrogen bond that is linked to the hydroxyl group of hydroxyectoine. In EhuB the same hydroxyl group is bound to Glu134, which seems to take over a crucial role in the high-affinity binding of hydroxyectoine. This was shown by the replacement of Glu134 for Ala134, which abolished any detectable hydroxyectoine binding to EhuB. The binding pocket of TeaA employing solvent interaction and direct amino acid interaction in binding ectoine makes TeaA a highly specific binding protein. However, while TeaA displays a higher affinity to ectoine than EhuB, the affinity to hydroxyectoine is comparatively low. Interestingly, NMR measurements revealed that hydroxyectoine in aqueous solution is existent in half-chair conformation with an axial hydroxyl group (*57*). Bound to EhuB and TeaA, however, hydroxyectoine was displaying a flipped conformation with an equatorial hydroxyl group.

It is tempting to speculate whether Glu134 in the binding pocket of EhuB is promoting the conformational change and allows for the better binding of hydroxyectoine compared to ectoine. Apparently, the solvent molecules in the TeaA binding pocket do not support binding of hydroxyectoine in the same way as Glu134 does in EhuB. However, missing the corresponding amino acid to Glu134, TeaA displays a significantly higher affinity for ectoine than EhuB. The negative influence of Glu134 on the binding of ectoine was also shown for EhuB. Replacing Glu134 for alanine increased the binding affinity of EhuB for ectoine to 1.2 μM. Thus the ability of TeaA to bind ectoine with high affinity is based on the reduced affinity for hydroxyectoine.

CONCLUSION

The structure of TeaA is a fundamental contribution toward defining the important parameters for an efficient osmoregulated compatible solute transport mediated by SBPs. Contrary to the common opinion that SBPs specific for the same substrate have to exhibit an identical architecture, the comparison of EhuB and TeaA revealed a different architecture of the binding site and the potential interaction regions of the SBPs with their corresponding transporters. Whether these differences originate from the fact that EhuB and TeaA belong to transporter systems, which have two completely different ways to energize the transport, one by ATP hydrolysis, the other by the electrochemical gradient across the membrane, can only be speculated. As a matter of fact, the choice of an organism for either an osmoregulated TRAP transporter or an ABC transporter clearly depends on the environmental conditions; e.g., TRAP-T that are ion coupled are preferably found in marine and halophilic bacteria with excess of environmental Na^+ (*20*). An increased substrate affinity of osmoregulated TRAP-T over conventional secondary transporters and the role of SBPs as an efficiency enhancer can be postulated but has to be proven by uptake measurements in vitro.

In the soil bacterium *S. meliloti*, the osmoprotectant transport differs from that observed in *H. elongata*. The EhuABCD transporter is responsible for the main ectoine transport activity observed in *S. meliloti* showing an ectoine transport activity that is induced only by its substrates ectoine and hydroxyectoine but not by elevated osmolality (*29*). Ectoine is not accumulated within the cell but rather is degraded at all medium osmolalities (*29*). The mechanism

by which ectoine overcomes osmotic growth inhibition remains unknown. The role of Ehu in osmoregulation is therefore quite different from other compatible solute transporters and more similar to nutrient transporters. Contrary to Ehu, the TeaABC system functions as an osmoregulatory uptake system for ectoine from the surrounding and as an effective salvage system for endogenous ectoine leaking through the membrane. The purpose of ectoine uptake via TeaABC is to amass ectoine in the cytoplasm in order to achieve an osmotic equilibrium. Furthermore, there is some evidence that TeaABC as a recovery system for ectoine might be involved in regulating ectoine synthesis. Since ectoine is the main compatible solute of *H. elongata*, the reuptake of ectoine for regulatory purposes would require a highly specific transporter. This would explain the 10 times higher affinity of TeaA for ectoine compared to EhuB. A similar conclusion can be drawn from the structural investigation of ProX from *E. coli* and ProX from *A. fulgidus*. ProU from *E. coli* accumulates glycine-betaine and proline-betaine as osmoprotectants, while ProU from *A. fulgidus* (*50*) transports the same molecules as thermoprotectants. Finally, it can be concluded that the affinity of the SBP is related to the importance of its respective transporter in cell regulatory processes.

ACKNOWLEDGMENT

We thank Werner Kühlbrandt (Frankfurt, MPI) for stimulating discussions, Míriel Teichmann for help in purification and crystallization, and Susanne Ressl, Sabrina Schulze, Tiago Barros, and Özkan Yildiz for collecting data, the latter also for help in data processing (all Frankfurt, MPI). We are grateful to the beam line staff at SLS PXII (Villigen, Switzerland) for excellent facilities and assistance.

REFERENCES

1. Sweeney, T. E., and Beuchat, C. A. (1993) Limitations of methods of osmometry: measuring the osmolality of biological fluids. *Am. J. Physiol. 264*, R469–R480.
2. Ventosa, A., Nieto, J. J., and Oren, A. (1998) Biology of moderately halophilic aerobic bacteria. *Microbiol. Mol. Biol. Rev. 62*, 504–544.
3. Kempf, B., and Bremer, E. (1998) Uptake and synthesis of compatible solutes as microbial stress responses to high-osmolality environments. *Arch. Microbiol. 170*, 319–330.
4. Martin, D. D., Ciulla, R. A., and Roberts, M. F. (1999) Osmoadaptation in archaea. *Appl. Environ. Microbiol. 65*, 1815–1825.
5. Kunte, H. J. (2006) Osmoregulation in Bacteria: Compatible Solute Accumulation and Osmosensing. *Environ. Chem. 3*, 94–99.
6. Brown, A. D. (1976) Microbial water stress. *Bacteriol. Rev. 40*, 803–846.
7. Bolen, D. W. (2004) Effects of naturally occurring osmolytes on protein stability and solubility: issues important in protein crystallization. *Methods Macromol. Crystal. 34*, 312–322.
8. Bolen, D. W., and Baskakov, I. V. (2001) The osmophobic effect: natural selection of a thermodynamic force in protein folding. *J. Mol. Biol. 310*, 955–963.
9. Severin, J., Wohlfarth, A., and Galinski, E. A. (1992) The predominant role of recently discovered tetrahydropyrimidines for the osmoadaptation of halophilic eubacteria. *J. Gen. Microbiol. 138*, 1629–1638.
10. Lentzen, G., and Schwarz, T. (2006) Extremolytes: natural compounds from extremophiles for versatile applications. *Appl. Microbiol. Biotechnol. 72*, 623–634.
11. Kanapathipillai, M., Lentzen, G., Sierks, M., and Park, C. B. (2005) Ectoine and hydroxyectoine inhibit aggregation and neurotoxicity of Alzheimer's β-amyloid. *FEBS Lett. 579*, 4775–4780.
12. Vreeland, R. H., Litchfield, C. D., Martin, E. L., and Elliot, E. (1980) *Halomonas elongata*, a new genus and species of extremely salt-tolerant bacteria. *Int. J. Syst. Bacteriol. 30*, 485–495.
13. Göller, K., Ofer, A., and Galinski, E. A. (1998) Construction and characterization of an NaCl-sensitive mutant of *Halomonas elongata* impaired in ectoine biosynthesis. *FEMS Microbiol. Lett. 161*, 293–300.
14. Peters, P., Galinski, E. A., and Trueper, H. G. (1990) Characterization of genes for the biosynthesis of the compatible solute ectoine from *Marinococcus halophilus* and osmoregulated expression in *Escherichia coli*. *Microbiology 143*, 1141–1149.
15. Bursy, J., Pierik, A. J., Pica, N., and Bremer, E. (2007) Osmotically induced synthesis of the compatible solute hydroxyectoine is mediated by an evolutionarily conserved ectoine hydroxylase. *J. Biol. Chem. 282*, 31147–31155.
16. Louis, P., and Galinski, E. A. (1997) Characterization of genes for the biosynthesis of the compatible solute ectoine from *Marinococcus halophilus* and osmoregulated expression in *Escherichia coli*. *Microbiology 143* (Part 4), 1141–1149.
17. Kunte, H. J. (2004) Transport and Accumulation of Osmoregulatory Solutes in *Bacteria*: Characterization of Transport-Systems and Their Regulatory Mechanisms in *Halomonas elongata, Marinococcus halophilus*, and *Escherichia coli*, Habilitationsschrift, Rheinische Friedrich-Wilhelms-Universität, Bonn, Germany.
18. Grammann, K., Volke, A., and Kunte, H. J. (2002) New type of osmoregulated solute transporter identified in halophilic members of the bacteria domain: TRAP transporter TeaABC mediates uptake of ectoine and hydroxyectoine in *Halomonas elongata* DSM 2581^T. *J. Bacteriol. 184*, 3078–3085.
19. Forward, J. A., Behrendt, M. C., Wyborn, N. R., Cross, R., and Kelly, D. J. (1997) TRAP transporters: a new family of periplasmic solute transport systems encoded by the *dctPQM* genes of *Rhodobacter capsulatus* and by homologs in diverse gram-negative bacteria. *J. Bacteriol. 179*, 5482–5493.
20. Mulligan, C., Kelly, D. J., and Thomas, G. H. (2007) Tripartite ATP-independent periplasmic transporters: application of a relational database for Genome-Wide Analysis of Transporter Gene Frequency and Organization. *J. Mol. Microbiol. Biotechnol. 12*, 218–226.
21. Rabus, R., Jack, D. L., Kelly, D. J., and Saier, M. H. (1999) TRAP transporters: An ancient family of extracytoplasmic solute-receptor-dependent secondary active transporters. *Microbiology 145*, 3431–3445.
22. Tetsch, L., and Kunte, H. J. (2002) The substrate-binding protein TeaA of the osmoregulated ectoine transporter TeaABC from *Halomonas elongata*: purification and characterization of recombinant TeaA. *FEMS Microbiol. Lett. 211*, 213–218.
23. Jacobs, M. H. J., van der Heide, T., Driessen, A. J. M., and Konings, W. N. (1996) Glutamate transport in *Rhodobacter sphaeroides* is mediated by a novel binding protein-dependent secondary transport system. *Proc. Natl. Acad. Sci. U.S.A. 93*, 12786–12790.
24. Driessen, A. J., Rosen, B. P., and Konings, W. N. (2000) Diversity of transport mechanisms: common structural principles. *Trends Biochem. Sci. 25*, 397–401.
25. Müller, A., Severi, E., Mulligan, C., Watts, A. G., Kelly, D. J., Wilson, K. S., Wilkinson, A. J., and Thomas, G. H. (2006) Conservation of structure and mechanism in primary and secondary transporters exemplified by SiaP, a sialic acid binding virulence factor from *Haemophilus influenzae*. *J. Biol. Chem. 281*, 22212–22222.
26. Rucktooa, P., Antoine, R., Herrou, J., Huvent, I., Locht, C., Jacob-Dubuisson, F., Villeret, V., and Bompard, C. (2007) Crystal structures of two *Bordetella pertussis* periplasmic receptors contribute to defining a novel pyroglutamic acid binding DctP subfamily. *J. Mol. Biol. 370*, 93–106.
27. Gonin, S., Arnoux, P., Pierru, B., Lavergne, J., Alonso, B., Sabaty, M., and Pignol, D. (2007) Crystal structures of an extracytoplasmic solute receptor from a TRAP transporter in its open and closed forms reveal a helix-swapped dimer requiring a cation for alpha-keto acid binding. *BMC Struct. Biol. 7*, 11.
28. Takahashi, H., Inagaki, E., Kuroishi, C., and Tahirov, T. H. (1846) (2004) Structure of the *Thermus thermophilus* putative periplasmic glutamate/glutamine-binding protein. *Acta Crystallogr., Sect. D: Biol. Crystallogr. 60*, 1854.
29. Jebbar, M., Sohn-Bosser, L., Bremer, E., Bernard, T., and Blanco, C. (2005) Ectoine-induced proteins in *Sinorhizobium meliloti* include an ectoine ABC-type transporter involved in osmoprotection and ectoine catabolism. *J. Bacteriol. 187*, 1293–1304.

30. Hanekop, N., Hoing, M., Sohn-Bosser, L., Jebbar, M., Schmitt, L., and Bremer, E. (2007) Crystal structure of the ligand-binding protein EhuB from *Sinorhizobium meliloti* reveals substrate recognition of the compatible solutes ectoine and hydroxyectoine. *J. Mol. Biol. 374*, 1237–1250.
31. Kunte, H. J., and Galinski, E. A. (1995) Transposon mutagenesis in halophilic eubacteria: conjugal transfer and insertion of transposon Tn5 and Tn1732 in *Halomonas elongata*. *FEMS Microbiol. Lett. 128*, 293–299.
32. Wiseman, T., Willistan, S., Brandts, J. F., and N., L. L. (1989) Rapid measurement of binding constants and heats of binding using a new titration calorimeter. *Anal. Biochem. 179*, 131–137.
33. Kabsch, W. (1993) Automatic processing of rotation diffraction data from crystals of initially unknown symmetry and cell constants. *J. Appl. Crystallogr. 26*, 795–800.
34. Pape, T., and Schneider, T. R. (2004) HKL2MAP: a graphical user interface for phasing with SHELX programs. *J. Appl. Crystallogr. 37*, 843–844.
35. Vonrhein, C., Blanc, E., Roversi, P., and Bricogne, G. (2006) Automated structure solution with autoSHARP. *Methods Mol. Biol. 364*, 215–230.
36. Cohen, S. X., Morris, R. J., Fernandez, F. J., Ben Jelloul, M., Kakaris, M., Parthasarathy, V., Lamzin, V. S., Kleywegt, G. J., and Perrakis, A. (2004) Towards complete validated models in the next generation of ARP/wARP. *Acta Crystallogr., Sect. D: Biol. Crystallogr. 60*, 2222–2229.
37. Murshudov, G. N., Vagin, A. A., and Dodson, E. J. (1997) Refinement of macromolecular structures by the maximum-likelihood method. *Acta Crystallogr., Sect. D: Biol. Crystallogr. 53*, 240–255.
38. C, P. N. (1994) The CCP4 Suite: Programs for protein crystallography. *Acta Crystallogr., Sect. D: Biol. Crystallogr. 50*, 760–763.
39. Ciulla, R. A., Diaz, M. R., Taylor, B. F., and Roberts, M. F. (1997) Organic osmolytes in aerobic bacteria from Mono Lake, an alkaline, moderately hypersaline environment. *Appl. Environ. Microbiol. 63*, 220–226.
40. DeLano, W. L. The PyMOL Molecular Graphics System, Delano Scientific LLC, San Carlos, CA (http://www/pymol.org).
41. Holm, L., and Sander, C. (1997) Dali/FSSP classification of three-dimensional protein folds. *Nucleic Acids Res. 25*, 231–234.
42. Kabsch, W. (1976) A solution for the best rotation to relate two sets of vectors. *Acta Crystallogr. 32*, 922–923.
43. Altschul, S. F., Gish, W., Miller, W., Myers, E. W., and Lipman, D. J. (1990) Basic local alignment search tool. *J. Mol. Biol. 215*, 403–410.
44. Thompson, J. D., Higgins, D. G., and Gibson, T. J. (1994) CLUSTAL W: improving the sensitivity of progressive multiple sequence alignments through sequence weighting, position specific gap penalties and weight matrix choice. *Nucleic Acids Res. 22*, 4673–4680.
45. Bioedit (http://www.mbio.ncsu.edu/BioEdit/bioedit.html).
46. Gouet, P., Robert, X., and Courcelle, E. (2003) ESPript/ENDscript: Extracting and rendering sequence and 3D information from atomic structures of proteins. *Nucleic Acids Res. 31*, 3320–3323.
47. Fukuchi, S., Yoshimune, K., Wakayama, M., Moriguchi, M., and Nishikawa, K. (2003) Unique amino acid composition of proteins in halophilic bacteria. *J. Mol. Biol. 327*, 347–357.
48. Bohm, G., and Jaenicke, R. (1994) A structure-based model for the halophilic adaptation of dihydrofolate reductase from *Halobacterium volcanii*. *Protein Eng. 7*, 213–220.
49. Mevarech, M., Frolow, F., and Gloss, L. M. (2000) Halophilic enzymes: proteins with a grain of salt. *Biophys. Chem. 86*, 155–164.
50. Dym, O., Mevarech, M., and Sussman, J. L. (1995) Structural features that stabilize halophilic malate dehydrogenase from an *Archaebacterium*. *Science 267*, 1344–1346.
51. Elcock, A. H., and McCammon, J. A. (1998) Electrostatic contributions to the stability of halophilic proteins. *J. Mol. Biol. 280*, 731–748.
52. Coronado, M. J., Vargas, C., Mellado, E., Tegos, G., Drainas, C., Nieto, J. J., and Ventosa, A. (2000) The alpha-amylase gene *amyH* of the moderate halophile *Halomonas meridiana*: cloning and molecular characterization. *Microbiology 146* (Part 4), 861–868.
53. Felder, C. B., Graul, R. C., Lee, A. Y., Merkle, H. P., and Sadee, W. (1999) The Venus flytrap of periplasmic binding proteins: an ancient protein module present in multiple drug receptors. *AAPS Pharm. Sci. 1*, E2.
54. Fukami-Kobayashi, K., Tateno, Y., and Nishikawa, K. (2003) Parallel evolution of ligand specificity between LacI/GalR family repressors and periplasmic sugar-binding proteins. *Mol. Biol. Evol. 20*, 267–277.
55. Schiefner, A., Holtmann, G., Diederichs, K., Welte, W., and Bremer, E. (2004) Structural basis for the binding of compatible solutes by ProX from the hyperthermophilic archaeon *Archaeoglobus fulgidus*. *J. Biol. Chem. 279*, 48270–48281.
56. Schiefner, A., Breed, J., Bosser, L., Kneip, S., Gade, J., Holtmann, G., Diederichs, K., Welte, W., and Bremer, E. (2004) Cation-pi interactions as determinants for binding of the compatible solutes glycine betaine and proline betaine by the periplasmic ligand-binding protein ProX from *Escherichia coli*. *J. Biol. Chem. 279*, 5588–5596.
57. Galinski, E. A. (1992) Kompatible Solute aus Bakterien—Gewinnung, Anwendung, Struktur und Funktion, Habilitationsschrift, Rheinische Friedrich-Wilhelms-Universität, Bonn, Germany.

BI8006719